Weber *et al. Molecular Autism* (2024) 15:38
https://doi.org/10.1186/s13229-024-00616-2

Molecular Autism

RESEARCH Open Access

Contracted functional connectivity profiles in autism

Clara F. Weber[1,2,3], Valeria Kebets[1], Oualid Benkarim[1], Sara Lariviere[1], Yezhou Wang[1], Alexander Ngo[1], Hongxiu Jiang[1], Xiaoqian Chai[4], Bo-yong Park[5,6], Michael P. Milham[7], Adriana Di Martino[7], Sofie Valk[8], Seok-Jun Hong[6,7,9,10] and Boris C. Bernhardt[1*]

Abstract

Objective Autism spectrum disorder (ASD) is a neurodevelopmental condition that is associated with atypical brain network organization, with prior work suggesting differential connectivity alterations with respect to functional connection length. Here, we tested whether functional connectopathy in ASD specifically relates to disruptions in long- relative to short-range functional connections. Our approach combined functional connectomics with geodesic distance mapping, and we studied associations to macroscale networks, microarchitectural patterns, as well as socio-demographic and clinical phenotypes.

Methods We studied 211 males from three sites of the ABIDE-I dataset comprising 103 participants with an ASD diagnosis (mean ± SD age = 20.8 ± 8.1 years) and 108 neurotypical controls (NT, 19.2 ± 7.2 years). For each participant, we computed cortex-wide connectivity distance (CD) measures by combining geodesic distance mapping with resting-state functional connectivity profiling. We compared CD between ASD and NT participants using surface-based linear models, and studied associations with age, symptom severity, and intelligence scores. We contextualized CD alterations relative to canonical networks and explored spatial associations with functional and microstructural cortical gradients as well as cytoarchitectonic cortical types.

Results Compared to NT, ASD participants presented with widespread reductions in CD, generally indicating shorter average connection length and thus suggesting reduced long-range connectivity but increased short-range connections. Peak reductions were localized in transmodal systems (i.e., heteromodal and paralimbic regions in the prefrontal, temporal, and parietal and temporo-parieto-occipital cortex), and effect sizes correlated with the sensory-transmodal gradient of brain function. ASD-related CD reductions appeared consistent across inter-individual differences in age and symptom severity, and we observed a positive correlation of CD to IQ scores.

Limitations Despite rigorous harmonization across the three different acquisition sites, heterogeneity in autism poses a potential limitation to the generalizability of our results. Additionally, we focussed male participants, warranting future studies in more balanced cohorts.

*Correspondence:
Boris C. Bernhardt
boris.bernhardt@mcgill.ca

Full list of author information is available at the end of the article

Conclusions Our study showed reductions in CD as a relatively stable imaging phenotype of ASD that preferentially impacted paralimbic and heteromodal association systems. CD reductions in ASD corroborate previous reports of ASD-related imbalance between short-range overconnectivity and long-range underconnectivity.

Keywords Autism spectrum disorder, Magnetic resonance imaging, Functional connectivity, Neurodevelopmental disorders, Distance profiling, Connectivity disruptions

Background

Autism spectrum disorder (ASD) is a prevalent neurodevelopmental condition [1, 2], commonly manifesting in atypical social cognition and communication, repetitive behaviors and interests, sometimes together with imbalances in affective, sensory, and perceptual processing [2–4]. Despite extensive research, pathomechanisms of ASD remain incompletely understood. Convergent evidence from molecular, histological, and neuroimaging work suggests atypical brain network organization, motivating continued efforts to identify substrates of autism connectopathy [5–10].

By interrogating brain structure and function in vivo, magnetic resonance imaging (MRI) lends itself as a window into the human connectome [11, 12]. Resting-state functional MRI (rs-fMRI) [13–16] can probe whole-brain intrinsic functional networks [17–20], both in terms of functionality and spatial layout [21–25]. Moreover, rs-fMRI analysis has become common in the study of typical and atypical neurodevelopment [5, 25, 26], and in identifying substrates of symptom profiles in complex neurodevelopmental conditions such as ASD [25, 27–30]. Across the cortex, there is an important inter-regional variability of functional connection length: patterns of strong local connectivity are typical for unimodal areas, including the somatosensory and visual systems, where fast and efficient local signal transmission is necessary [23, 31]. Contrarily, long-range connections are increasingly found in heteromodal association systems and paralimbic networks, systems that implicate more integrative, cognitive-related processing [31, 32]. While longer connections are metabolically expensive to build and maintain [31, 33], they conversely provide gains in terms of processing flexibility and integrative capacity [23, 31, 32].

Increasing evidence suggests widespread functional connectivity alterations in ASD, generally reporting mosaic patterns of under- and overconnectivity in ASD as compared to neurotypical controls (NT) [5, 34–37]. In individuals with ASD, short- and long-range connectivity is likely affected differently [34, 38]. While underconnectivity in ASD is reported at a global level and in transmodal systems, such as the default mode network (DMN) [5, 35, 39], there is some literature also emphasizing overconnectivity in the condition, primarily in unimodal cortical areas and subcortico-cortical networks [9, 35, 40]. Of note, atypical connectivity has been shown to vary with inter-individual differences and potential ASD subtypes [29, 41, 42]. It has been hypothesized that ASD is associated with long-range underconnectivity, but short-range overconnectivity [38, 43, 44]. However, as studies report diverging results, existing evidence fails to provide a comprehensive and mechanistic explanation and spatial mapping of ASD-related connectivity alterations. Associations between connectivity alterations, on the one hand, and phenotype variations as well as developmental mechanisms, on the other hand, remain to be established as well [45, 46]. Functional connectivity and distance length are spatially linked, as long- and short-range connections are neither randomly nor evenly distributed across the cortex, but characteristic connection length of a cortical region mirrors its position in the putative cortical hierarchy [31, 32]. Thus, combining functional neuroimaging and topological information can provide further insights into connectivity shifts in ASD. Previous studies have proposed connectivity distance (CD) as a metric that combines functional connectivity with measures of spatial proximity between brain areas [31, 38, 47], notably with geodesic distance between areas along the cortical surface [47, 48]. CD is the average distance to connected nodes of a given vertex, thus capturing functionally relevant connection lengths [31, 47]. In NT populations, CD has been found to increase with distance to primary cortical areas [31], supporting that short-range connections predominate in unimodal regions while long-range connections are increasingly present in transmodal association systems, such as the DMN. Additional evidence has underlined impaired segregation and integration between cortical hierarchies in ASD mirrored in functional neuroimaging [49].

The recognized etiological heterogeneity in ASD motivates contextualization of neuroimaging-based phenotypes against established measures of neural organization, to explore potential pathways of susceptibility. Converging evidence hints towards a relationship between CD and cortical microarchitecture [31, 32, 47, 50, 51], notably cellular composition, columnar topography, and lamination of the cortex [50, 52]. Local increases in cell density and smaller pyramidal cells [53–55], suggestive of short-range overconnectivity at the expense of long-range connections, could potentially impact macro-level connections and circuit function [54, 56]. Neuronal cell size, density, and connection types vary across cortical areas and their modalities, as observed in histological

studies as early as in the foundational descriptions of cortical types [57]. The microstructural organization of the cortex is generally thought to correlate with large-scale functional organization, with unimodal regions exhibiting stronger lamination patterns while transmodal systems express reduced laminar differentiation [58]. More recently, analyzing *post mortem* histological reconstructions of the human brain has allowed for additional histological contextualization of imaging findings [59–63]. In particular, the 3D BigBrain dataset has been used to derive microstructural cortical gradients that run from sensory to paralimbic systems [64]. Despite some differences [64, 65], this hierarchical axis is largely converging with descriptions of the functional cortical hierarchy [23], and decompositions of resting-state functional connectivity [24, 66, 67]. As such, these resources set the stage to explore whether connectome contractions in ASD follow microstructural and functional gradients, indicating a connectopathological susceptibility aligning with cortical hierarchical organization. In this study, we thus aim to extend and build upon previous description of atypical functional connectivity [9, 11, 43] and atypical functional network hierarchy in ASD [25], by specifically interrogating shifts in connectivity distances in ASD.

Considering the mounting evidence of the differential impact of long- vs. short-range connectivity alterations in ASD, we aimed to investigate CD in individuals with ASD and NT as a possible underpinning of shorter average connection length, i.e. contracted connectome profiles in ASD. We leveraged the multi-centric Autism Brain Imaging Data Exchange (ABIDE-I) repository [68] and quantified CD alterations in ASD relative to NT by combining rs-fMRI connectivity analysis with cortex-wide geodesic distance mapping. We contextualized ASD-related CD reductions across functional networks and sensory-transmodal gradients of cortical functional hierarchy [24]. On a microscopic scale, we investigated correlation to histology-derived gradient maps and cortical types, to find a more complete explanatory model for connectome contractions in ASD.

Methods

Participants

We studied data from the first release of the Autism Brain Imaging Data Exchange (ABIDE) [68], a multicentric data and imaging collection consortium. Similar to previous work [25, 69, 70], we included imaging and clinical data from three different sites that included data from >=10 ASD and NT respectively, i.e., University of Pittsburgh School of Medicine (PITT), New York University Langone Medical Center (NYU), and University of Utah School of Medicine (USM). ABIDE data has been collected in alignment with local institutional review board frameworks and made publicly available in an anonymized form in accordance with the Health Insurance Portability and Accountability Act (HIPAA) guidelines. ASD individuals were identified in an in-person diagnostic interview using the Autism Diagnostic Observation Schedule (ADOS), and subjects with genetic disorders associated to ASD, or contraindications to scanning such as pregnancy were excluded from the study. NT controls did not have any history of psychiatric disease. Due to the small number of female participants included in the first ABIDE release [68], we limited our analysis to male individuals. Additionally, we only retained cases with acceptable T1-weighted imaging quality and surface extraction outcomes. After excluding cases with high head motion (cutoff: >2SD over mean framewise displacement, $n=10$), we obtained a sample size of $n=211$ (103/108 ASD/NT). Frame censoring was not performed. To assess symptom severity, we considered ADOS scores [4], which evaluate three characteristic symptomatic domains of ASD, i.e., communication and language, reciprocal social interactions and restricted/repetitive behaviors. Furthermore, we considered intelligence quotient (IQ) and IQ subscores for verbal and performance IQ as measured by the Wechsler Adult Intelligence Scale [71]. Since previous literature suggests cognitive imbalances, such as high variability between verbal and nonverbal abilities, in ASD [72, 73], we additionally calculated and analyzed the ratio of verbal over nonverbal IQ [74]. Detailed demographic information is provided in Table 1.

MRI acquisition parameters

Data from all three sites were acquired on 3T Siemens scanners. Acquisition protocols for T1-weighted (T1w) and rs-fMRI were as follows for the three included sites: *(i) NYU.* Data were acquired on Allegra scanner using 3D-TurboFLASH for T1w (repetition time (TR)=2530 ms; echo time (TE)=3.25 ms; inversion time (TI)=1100 ms; flip angle=7°; matrix=256×256; 1.3×1.0×1.3 mm^3 voxels) and 2D-echo planar imaging (EPI) for rs-fMRI (TR=2000ms; TE=15 ms; flip angle=90°; matrix=80×80; 180 volumes, 3.0×3.0×4.0 mm^3 voxels); *(ii) PITT.* Data were acquired on an Allegra scanner using 3D-MPRAGE for T1w (TR=2100 ms; TE=3.93 ms; TI=1000 ms; flip angle=7°; matrix=269×269; 1.1×1.1×1.1 mm^3 voxels) and 2D-EPI for rs-fMRI (TR=1500 ms; TE=35 ms; flip angle=70°; matrix=64×64; 200 volumes, 3.1×3.1×4.0 mm^3 voxels); *(iii) USM.* Data were acquired on a TrioTim scanner using 3D-MPRAGE for T1w (TR=2300 ms; TE=2.91 ms; TI=900 ms; flip angle=9°; matrix=240×256; 1.0×1.0×1.2 mm^3 voxels) and 2D-EPI for rs-fMRI (TR=2000ms; TE=28 ms; flip angle=90°; matrix=64×64; 240 volumes; 3.4×3.4×3.0 mm^3 voxels).

Table 1 Study cohort demographic information for ASD and neurotypical control (NT) groups. Age in years (y), SD = standard deviation

Group	ASD		NT
n	103		108
Mean Age (SD) [y]	20.842 (8.112)		19.220 (7.103)
Mean IQ (SD)	104.359 (15.734)		114.176 (12.310)
Mean Verbal IQ (SD)	101.767 (16.823)		113.269 (12.541)
Mean Performance IQ (SD)	105.903 (15.623)		111.833 (12.489)
Mean IQ Ratio (V/Q) (SD)	0.972 (0.167)		1.020 (0.121)
Mean ADOS (SD)	12.612 (3.734)		-
Mean ADOS Communication (SD)	4.243 (1.531)		-
Mean ADOS Social Interaction (SD)	8.369 (2.683)		-
Mean ADOS Repetitive Behavior (SD)	2.029 (1.485)		-
Site	**PITT**	**NYU**	**USM**
n(ASD)/n(NT)	19/20	35/51	49/37
Mean Age (SD) for ASD/NT [y]	20.595 (7.416)/19.618 (6.489)	16.841 (7.536)/17.512 (6.730)	23.795 (7.642)/21.258 (7.479)
Mean ADOS (SD)	12.684 (3.127)	11.286 (4.191)	13.531 (3.373)
Mean ADOS Communication (SD)	4.211 (1.084)	3.629 (1.646)	4.694 (1.461)
Mean ADOS Social Interaction (SD)	8.474 (2.366)	7.657 (2.980)	8.837 (2.511)
Mean ADOS Repetitive Behavior (SD)	2.737 (1.195)	2.057 (1.083)	1.735 (1.741)
Mean IQ (SD) ASD/NT	112.316 (13.634)/110.250 (8.559)	105.286 (13.768)/114.961 (12.091)	100.612 (16.794)/115.216 (14.075)
Mean Verbal IQ (SD) ASD/NT	109.842 (12.208)/108.35 (10.479)	104.171 (14.168)/114.824 (12.106)	96.918 (18.689)/113.784 (13.742)
Mean Performance IQ (SD) ASD/NT	111.263 (14.185)/109.150 (8.015)	105.343 (13.750)/111.608 (13.180)	104.225 (17.171)/113.595 (13.459)
Mean IQ Ratio (V/Q) (SD) ASD/NT	0.999 (0.151)/0.996 (0.099)	0.998 (0.141)/1.039 (0.142)	0.943 (0.188)/1.006 (0.098)

MRI Processing

a) Structural MRI processing. T1w data were preprocessed using FreeSurfer v5.1 [75–77] (https://surfer.nmr.mgh.harvard.edu), which included bias field correction, intensity normalization, removal of non-brain tissue, and white matter segmentation. For accurate gray/white matter separation and cortical modelling, a mesh model was fit onto the white matter volume. Resulting surfaces were spherically aligned to a template based on sulco-gyral patterns.

b) Geodesic distance. We calculated geodesic distance as the physical distance of vertices along the pial surface. Specifically, we computed each individual's intra-hemispheric geodesic distance map between all pairs of vertices within each hemisphere, using the HCP Workbench *surface-geodesic-distance* command [78] (https://www.humanconnectome.org/software/workbench-command) and resampled data to Conte69 surface space to obtain 10,242 vertices per hemisphere [79] (https://github.com/Washington-University/HCPpipelines). Additionally, we extracted intracranial volume measures using FreeSurfer v5.1 [80]. Briefly, this approach leverages the registration matrix between an individual image to a standard atlas space to estimate intracranial volume [81, 82].

c) Resting-state fMRI processing. The rs-fMRI data were processed as described previously [49] based on the configurable pipeline for the analysis of connectomes (C-PAC) (https://fcp-indi.github.io/) [83], including slice-time and head motion correction, skull stripping and intensity normalization. Data were corrected for head motion, as well as white matter and cerebrospinal fluid signals using CompCor [84], followed by band-pass filtering (0.01–0.1 Hz). Both T1w and rs-fMRI data were linearly co-registered and mapped to MNI152 space. Functional imaging data were mapped to corresponding mid-thickness surfaces. We resampled data to the Conte69 surface template [79] via Workbench [78] with 10,242 surface points (vertices) per hemisphere. Due to the ongoing debate about global signal regression (GSR) [85], we did not apply GSR, but conducted additional control analyses using data that underwent GSR. We smoothed timeseries using a 5 mm full-width-at-half-maximum Gaussian kernel and computed intra-hemispheric functional connectivity (FC) as the Pearson correlation between all pairs of vertices within each hemisphere. FC matrices were Fisher r-to-z-transformed, to render correlation coefficients more normally distributed. Subjects with a mean framewise displacement (FD) > 0.3 mm in rs-fMRI (two SD from the mean across all subjects) were excluded (n = 9). Data were harmonized for site effects while preserving effects of age and ASD diagnosis using ComBat [86], which minimizes site-specific scaling factors by estimating their additive and multiplicative influence in a linear model, using empirical Bayes to predict site parameters more accurately [87, 88].

d) Connectivity distance profiling. We integrated FC and geodesic distance measures to compute CD profiles, as described previously [25, 47, 48]. Each participant's FC matrix was masked to only consider the 10% strongest (i.e., highest absolute) values per hemisphere.

This threshold was chosen as prior literature suggested potential bias towards inter-individual differences with stricter cutoffs, and corresponding loss of functional specificity with more lenient thresholds [31]. Previous literature applying similar methodology applied a similar cutoff [47, 48]. CD was computed by binarizing thresholded FC matrices and retrieving the row-wise average geodesic distance in these nodes, generating a single value per vertex for each participant. The resulting CD maps, thus, reflects the average distance on the cortex from each region to the areas to which it is strongly connected to, thereby combining anatomical and functional information.

Statistical analysis

We fit surface-based linear models correcting for age and head motion (as measured by mean framewise displacement) at each vertex *i*.

$$CD_i = ß_0 + ß_1 * Age + ß_2 * Diagnosis + ß_3 * Head\ Motion.$$

and group differences between ASD and NT were assessed in vertex-wise two-tailed Student's t-tests using the BrainStat toolbox (https://github.com/MICA-MNI/BrainStat) [60]. Additionally, we computed vertex-wise effect sizes using *Cohen's d*. Resulting *p*-values were adjusted for multiple comparisons using random field theory correction for non-isotropic images [89].

Several *post-hoc* analyses investigated the relationship between CD and behavioral metrics. Within ASD, we tested for associations to ASD symptom severity scores, specifically, total ADOS scores and ADOS subscores for communication, social interaction, and repetitive behaviors. In both ASD and NT groups, we examined the correlation to total IQ as well as verbal and performance IQ subscores, and the ratio of verbal and performance IQ [74]. First, we assessed the whole-brain association of CD with behavioral metrics in a vertex-wise linear model as described above. Additionally, we assessed the association to behavioral metrics within clusters of significant group differences which were identified in the previous step. Mean CD values were extracted from each cluster and the correlation to IQ and ADOS metrics were determined, adjusting for multiple comparisons using a false discovery rate (FDR) correction method [90].

Contextualization to macro- and microscale principles of cortical organization

We explored effect sizes for group differences between ASD and NT individuals, i.e. Cohen's *d*-values, and studied associations to macro- and microscale cortical patterns. For the whole-brain large-scale investigation, we analyzed mean CD and effect sizes in each of the seven previously described intrinsic functional networks [21]. Subsequently, we assessed the spatial correlation between Cohen's *d* effect sizes and scores of the principal functional gradient that describes sensory-transmodal functional differentiation [24], while accounting for spatial autocorrelation with 5000 spin permutations [91]. We similarly investigated effect sizes within cytoarchitectonic cortical types of Von Economo and Koskinas [57, 58] leveraging the ENIGMA toolbox [61]. Finally, we assessed associations to the BigBrain histology gradient that describes microstructural differentiation [92], again sourced from the ENIGMA toolbox [61].

Results

Reduced connectivity distance (CD) in autism

Mean CD in NT was higher within transmodal regions (i.e., heteromodal and paralimbic regions), such as the prefrontal and cingulate cortex and temporo-occipital-parietal junction, while CD values were lower in primary sensory and motor regions (Fig. 1A).

Comparing groups with linear models that additionally corrected for age and head motion revealed diffuse CD reductions in ASD relative to NT (Fig. 1B), with twelve clusters deemed significant after multiple comparisons correction (p_{RFT}<0.05). Clusters were mainly localized in the left and right temporal lobes and left prefrontal cortex (Figs. 1B and 2A). *Cohen's d* effect sizes for between-group differences amounted to d=0.600 in the temporal and left prefrontal cortex (Fig. 1B). Overall, there was a consistent shift of the CD distributions in ASD relative to NT across all significant clusters (Fig. 1C). Of note, CD was averaged per vertex, hence, the apparent decrease mirrors an increase in short-range connections at the expense of long-range links [47].

Effects of age, symptom severity and intelligence measures

Within clusters of significant ASD-related reductions identified in the vertex-wise model, there was no significant correlation to age (r=0.151, p_{FDR}=0.274, Table 2). Moreover, there were no between-group effects when comparing children and adults, which indicated that ASD-related CD reductions were stable across pediatric and adult cohorts (t=-0.469, p_{FDR}=0.640, Fig. 2B; Table 2).

Within clusters of significant between-group differences, CD in the ASD group also did not show any significant associations with ADOS symptom severity scores (r=0.047, p_{FDR}>0.4) nor with ADOS subscores for communication (r=0.028, p_{FDR}>0.4), social interaction (r=0.049, p_{FDR}=>0.4), and repetitive behaviors and interests (r=-0.037, p_{FDR}>0.4). On the other hand, when averaged within all clusters, there was a significant association of CD with full (r=0.324, p_{FDR}<0.001), verbal (r=0.304, p_{FDR}<0.001), and performance IQ (r=0.245, p_{FDR}=0.001; Table 2), while no significant interaction between diagnosis group and IQ measures was detectable (full IQ: r=-0.004, p_{FDR}=0.561, verbal IQ: r=0.005, p_{FDR}=0.561, performance IQ: r=-0.011, p_{FDR}=0.214, IQ

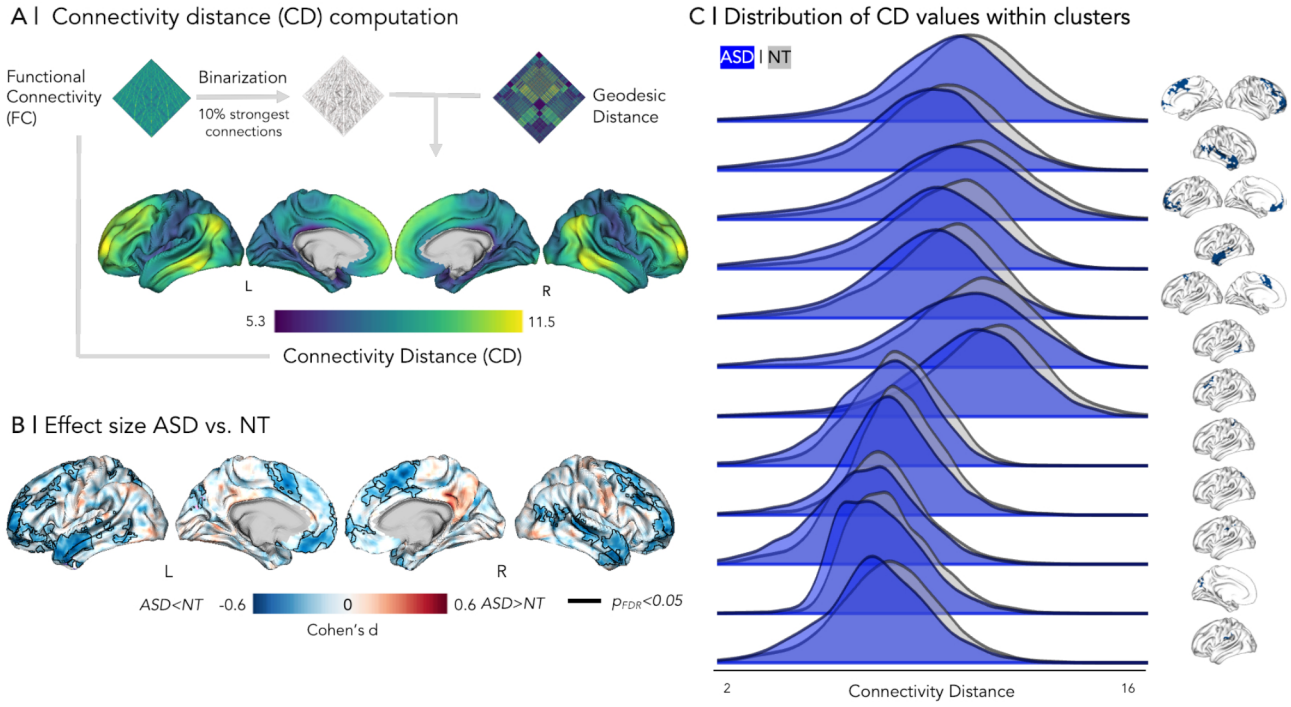

Fig. 1 **A** | Workflow for CD computation and average CD maps. **B |** Effect size map for group differences (ASD vs. NT). Clusters of significant changes after multiple comparisons correction are outlined (p_{FDR}<0.05, vertex-based linear model). **C |** Distribution of CD values within clusters of significant reduction

ratio: r=1.476, p_{FDR}=0.128). Similar results were obtained in cluster-wise analysis. Figure 2D-E shows correlation between behavioral metrics and mean CD across all clusters, while separate cluster-wise analyses can be found in Supplemental Fig. 2 & Supplemental Table 1.

In addition to cluster-wise analyses, we assessed whole-brain associations between CD and clinical metrics using a linear model of the influence of a behavioral score on CD while accounting for head motion and age. Overall, vertex-wise findings were consistent with within-cluster results (Supplemental Fig. 3).

Relation to cortical organization

Macroscale functional contextualization. Effect sizes differed across seven intrinsic functional networks [21], with higher effects towards transmodal compared to sensory/motor networks and peak reductions in CD in the limbic network (*Cohen's d*=-0.159, Fig. 3A). These findings were recapitulated when correlating effects against the intrinsic functional gradient [24] (r=-0.381, p_{spin}<0.001), which were significant even when using null models correcting for spatial autocorrelation (Fig. 3B).

Microstructural and cytoarchitectonic contextualization. For cortical types as proposed by Von Economo and Koskinas [58], we were able to see notable effect size variations that also became larger towards limbic/paralimbic regions, with highest effect sizes being present in agranular polar cortex (*Cohen's d*=0.201, Fig. 3C). On the other hand, effects sizes and the primary BigBrain microstructural gradient were not significantly correlated (r=-0.148, p_{spin}=0.265; Fig. 3D).

Control analyses

To ensure the robustness of our results across different data processing methods, we repeated analyses using functional connectivity that underwent GSR. Supplemental Fig. 1 shows respective effect size maps for both CD differences from uncorrected and from GSR-corrected functional CD maps. In both contrasts, highest between-group differences were localized in the left temporal lobe and left prefrontal cortex, as well as the right frontal lobe. However, group differences appeared higher for uncorrected data in medial prefrontal regions bilaterally, as well as the right temporal lobe. The congruence of both maps (r=0.546, p<0.001) suggested robustness of our results with respect to GSR application vs. omission during data preprocessing. There was no statistically significant difference in effect sizes between both approaches (t=-0.167, p_{FDR}=0.912).

To further characterize the thresholded FC matrices, we determined the correlation between triangular matrices of each participant in each group separately (mean±SD r_{ASD}=0.408±0.179, r_{NT}=0.414±0.141).

Moreover, we assessed intracranial volume and head motion as potential confounds for geodesic distance measures. There was no significant between-group difference in intracranial volume (t=0.694, p=0.488) or head motion (mean framewise displacement (FD): t=1.437,

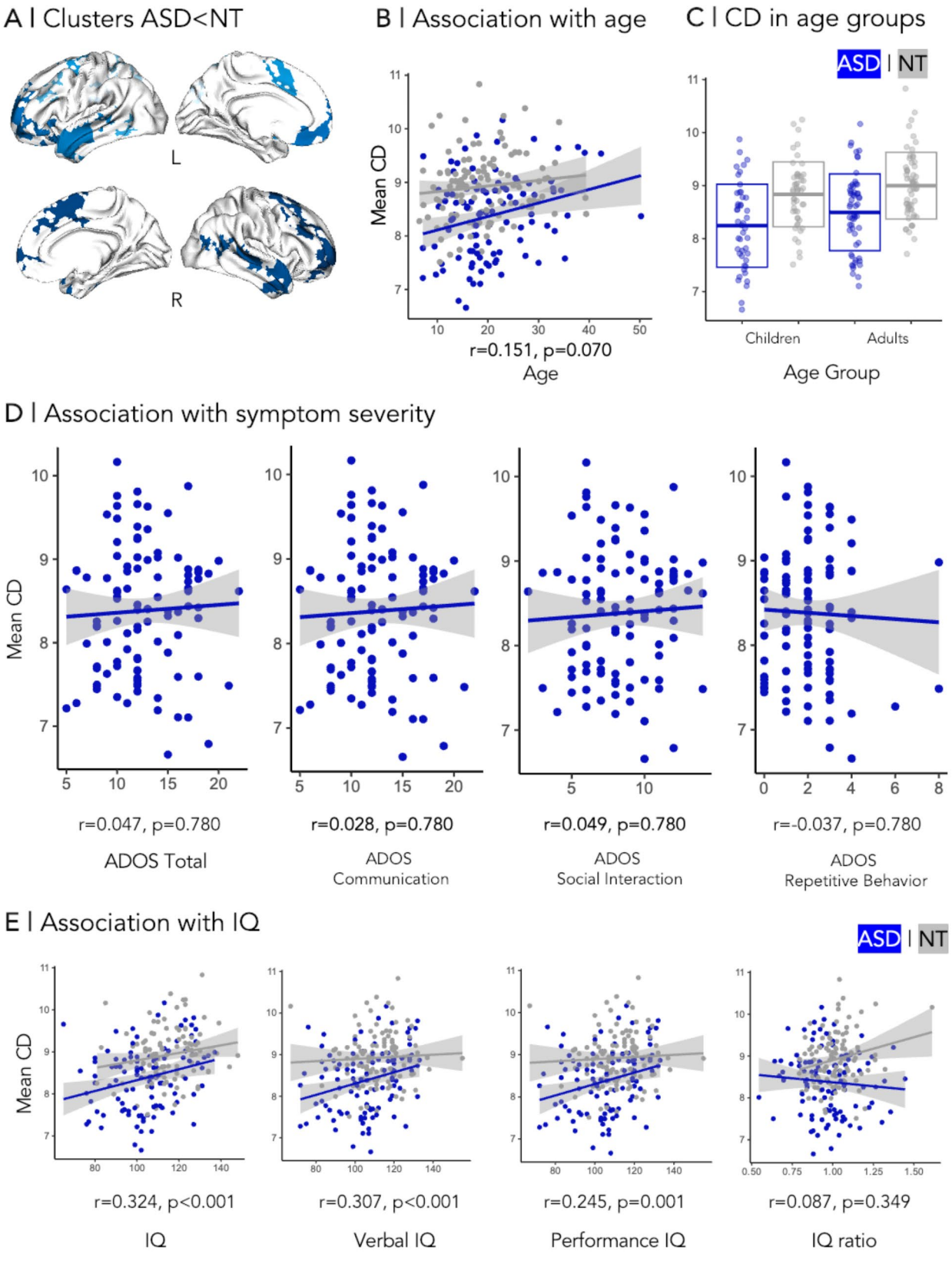

Fig. 2 **A |** Clusters of significant CD reduction in ASD vs. NT. Color intensity does not reflect effect size but as a visual differentiation between clusters. **B-E |** Correlation between mean CD in clusters and age, age group (children < 18 years, adults > 18 years), total ADOS score, ADOS subscores for communication, social interaction, and repetitive behavior, as well as full IQ and IQ subscores for verbal and nonverbal IQ. IQ ratio denotes the ratio of verbal over nonverbal IQ. Correlation coefficients are listed in Table 2

Table 2 Correlation between mean CD (CD) in clusters of significant group differences and age, age group (children < 18 years and adults > = 18 years) as well as behavioral metrics. *P*-values were corrected for multiple comparisons using false discovery rate correction (q < 0.05). Supplemental table 1 provides values for each of the twelve clusters separately

	Pearson's *r* (95% CI)	*p*
Age	0.151 (0.017–0.281)	0.070
ADOS Total	0.047 (-0.148–0.238)	0.780
ADOS Communication	0.028 (-0.167–0.22)	0.780
ADOS Social Interaction	0.049 (-0.146–0.24)	0.780
ADOS Repetitive Behavior	-0.037 (-0.229–0.158)	0.780
Full IQ	0.324 (0.197–0.44)	**< 0.001**
IQ ratio (Verbal/Nonverbal)	0.087 (-0.049–0.219)	0.349
Verbal IQ	0.307 (0.18–0.425)	**< 0.001**
Performance IQ	0.245 (0.114–0.368)	**0.001**

$p=0.152$). Of note, there were eminent site-related differences in ADOS scores, suggesting behavioral phenotype differences between the cohorts or variations in clinical symptom severity assessment ($F=3.904$, $p=0.023$, Supplemental Fig. 4A).

CD and group differences were largely congruent across sites, with some differences affecting occipital, opercular, and parietal regions (Supplemental Fig. 4B). To mitigate potential confounds relating to acquisition site, we utilized ComBat harmonization [88]. To ensure reliability, we compared results with those after site correction using a surface-based linear model. Resulting t-value maps from both approaches were highly congruent (r=-0.977, $p_{spin}<0.001$).

Finally, we tested the robustness of our results in CD across different FC thresholds. While our main approach considered the 10% strongest connection, we replicated our findings based on 5% and 20% FC thresholds. Both mean CD and effect size maps showed high congruence when compared to the main approach based on 10% FC (mean CD: $r=0.748$, $p_{spin}<0.001$; $r=0.676$, $p_{spin}<0.001$ respectively, Cohen's d: $r=0.968$, $p_{spin}<0.001$; $r=0.919$, $p_{spin}<0.001$ for 5%-CD and for 20%-CD respectively).

Discussion

Atypical brain connectivity is thought to be at the core of autism [93]. Here, we combined functional connectivity analysis with cortex-wide geodesic distance mapping to characterize shifts in the spatial extent of regional connectivity profiles [25, 47, 48]. Leveraging the open-access ABIDE dataset composed of ASD and NT individuals, we found robust evidence for global CD reductions in ASD, hinting towards a deficiency in long-range connections and a compensatory increase in short-range connectivity. Examining associations to functional topography, we noted a significant correlation to sensory-transmodal functional gradients, with most marked findings in paralimbic and heteromodal functional zones [24]. Likewise, contextualization against cytoarchitectural taxonomy [57, 58, 61] revealed most marked effects in

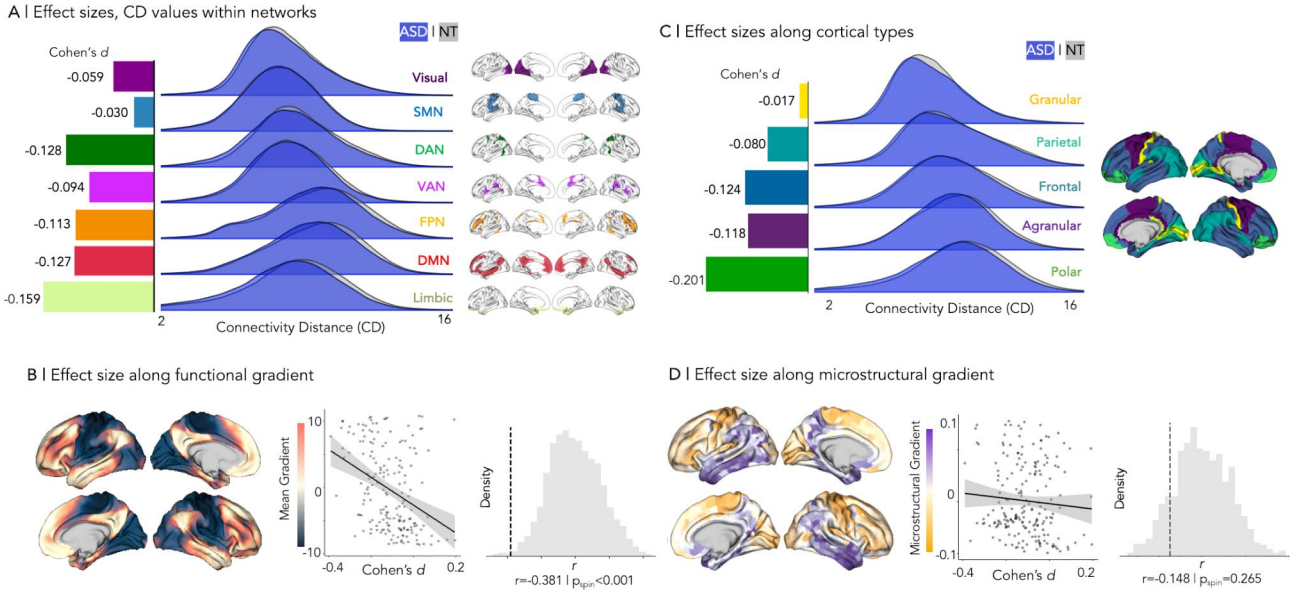

Fig. 3 Relation to cortical organization. **A |** Effect sizes of between-group differences (ASD vs. NT) in functional CD measures, stratified within seven intrinsic networks proposed by Yeo, Krienen, et al. [21] **B** | Correlation to the principal functional gradient [24]. Spatial associations were assessed using Spearman's rank test, and *p*-values were adjusted for spatial autocorrelation using a spin test [91, 129]. **C** | Effect size for the between-group difference in functional CD in each cortical type as proposed by Von Economo and Koskinas [58]. **D** | Association to microstructural gradients derived from the 3D BigBrain [59]. *Abbreviations*: SMN = somatomotor network, DAN = dorsal attention network, VAN = ventral attention network, FPN = frontoparietal network, DMN = default mode network

agranular and polar cortices with low laminar differentiation. Findings were relatively robust across FC thresholds employed in CD computation, and were consistent across the different sites and age strata included in the study. While findings were largely similar irrespective of using GSR during preprocessing, effect size maps from GSR-corrected CD exhibited a shift towards more positive values than those from non-corrected CD. As such, GSR appeared to be associated with farther distance between vertices in the ASD group relative to the NT group, potentially indicating a masking effect of global signals in short-range connections. CD reductions were stable across symptom severity metrics. While our findings did, thus, not capture imaging correlates of inter-individual differences in autism symptom load, these findings may suggest that CD reductions could constitute a stable imaging phenotype in neurodevelopmental conditions such as autism. On the other hand, CD alterations were positively correlated to both verbal and performance IQ measures, suggesting that these imbalances may index overall cognitive function in ASD. Collectively, imbalances in connectivity length distribution constitute a stable imaging phenotype of atypical neurodevelopment in ASD, with regional susceptibility intertwined with overarching principles of macroscale cortical organization.

The CD measure employed in this work combined rs-fMRI as an established in vivo proxy for functional interactions [94] with cortex-wide geodesic distance mapping [24, 47, 95, 96] to profile average functional connection length. This metric has been suggested to mirror functional and hierarchical properties of cortical areas, and to stratify systems in a data-driven, yet anatomically meaningful way [31, 32]. Previous work provided descriptions of atypical hierarchical cortical organization in ASD [25], which we have refined and expanded upon as part of the description of CD characteristics in ASD provided in the present article. Prior research and our current findings have consistently demonstrated that long-range cortico-cortical connections predominate in transmodal networks, which comprise heteromodal association systems such as the default mode network as well as paralimbic cortices [26, 39, 49]. These connections ensure efficient integration of functional signals in higher-order networks that are increasingly involved in abstract, integrative, as well as internally-generated cognitive and affective processes [16, 24, 97]. As CD reflects averaged distance values per each vertex, the measure remains somewhat opaque about the precise distribution of short- and long-range connections. Yet, the direction of findings as well as inspection of distributional histograms indicated shifts towards short-range links at the expense of long-range connections in ASD. The observed decrease in long-range connectivity in ASD in this study may indicate brain reorganization characterized by reduced inter-network connectivity together with compensatory strengthening of local connections [43]. The topography of CD changes in ASD may indeed be particularly meaningful in the context of cortical hierarchies, a conjecture supported by the macro- and microscale contextualization analyses conducted in the current work. Here, we observed a sensory-fugal pattern of ASD-related CD alterations when cross-referencing our findings to intrinsic functional measures. Specifically, we observed that ASD-related CD alterations mirrored the intrinsic functional gradient of information abstraction, which runs from primary input to unimodal regions to higher-level cognition in transmodal cortices [30, 49]. Stratifying findings across seven intrinsic networks derived in previous work [21], we also found the largest effect sizes in limbic networks, confirming that ASD-related CD alterations primarily affect paralimbic/fugal systems. While cross-referencing ASD-related effects to microstructure-based neural data did reveal a weak trend, however no significant association to this trajectory, cytoarchitecture type stratification of our in vivo imaging-derived metrics showed the strongest effect sizes in limbic agranular and polar cortices [57]. Of note, the lack of association to microstructural patterns as derived from the BigBrain gradient might originate from the current scarcity of different high-resolution histological datasets, and warrants confirmatory analysis upon the availability of aggregated histological data from multiple subjects.

Our findings demonstrated increased vulnerability for ASD-associated connection length contractions in heteromodal and paralimbic cortices that collectively make up the transmodal core of cortical organization [66, 98–100]. When considering anatomical but also functional connectivity relationships across the cortex, both paralimbic as well as heteromodal association cortices are situated at a high distance from primary sensory and motor regions interacting with the here and now [101, 102]. When considering cortical microarchitecture, particularly its laminar organization, there has been evidence for an axis that differentiates sensory/motor on the one end from paralimbic systems on the other end [62, 64, 103, 104]. These characteristics are highlighted in spatial variations in the visibility of the internal granular layer, commonly referred to as layer IV [101, 105, 106]. In effect, the agranular cortex lacks the respective layer, the dysgranular cortex exhibits rudimentary layer IV characteristics, and the granular cortex shows clear layer IV [101]. Limbic and paralimbic cortical systems comprise mainly the agranular and dysgranular extent of this spectrum [101, 102, 107]. As such, paralimbic systems are microstructurally most segregated from granular systems interacting with the external environment [64]. Converging, but also somewhat different from the microstructural gradient is the sensory-association

functional gradient, which radiates from sensory and motor systems towards heteromodal areas in the DMN [24, 64, 103]. These regions may contain complex microstructural signatures, including agranular types as well as granular cortices [23, 57, 58, 98]. In both heteromodal association systems as well as paralimbic cortices, there is prior evidence to suggest increased susceptibility to neurodevelopmental perturbations [62, 101]. Deficiency in long-range connectivity potentially results from cellular and laminar alterations [47], which may present a common substrate for different psychiatric and neurodevelopmental conditions [51, 62]. Risk genes for ASD as well as other neurodevelopmental conditions impact corticogenesis as early as in germinal stages [108, 109], impacting later axonal development that may disproportionally affect heteromodal systems [54, 110]. In future work, it remains thus to be established whether the current findings are specific to autism, or also visible in related neurodevelopmental indications. Our results, nevertheless, provide further justification to study microcircuit and macroscale alterations based on compact intermediary phenotypes such as CD. As such, they establish a perspective for future research, in order to better investigate and ultimately understand differentially impacted cortical hierarchies across common neurodevelopmental conditions.

Neuroimaging correlates of the typically developing connectome indicate marked shifts from local towards more distributed network patterns connections, while facilitating signaling across lobes and hemispheres [111, 112]. This progression highlights increased functional integration across brain networks, with short-range connections undergoing functional refinement [113, 114]. As such, network characteristics change from emphasized local processing in children to spatially and functionally distributed effects [112, 114, 115]. A potential microscale developmental mechanism driving this redistribution in typical development may be synaptic pruning [116–119]. In addition to its role in healthy brain maturation [120, 121], atypical pruning has been suggested in ASD [116, 122–124]. One common target of genetic alterations associated with increased risk for ASD are glutamergic synapses [125], which are involved in connection formation and pruning processes [117, 126]. Histological findings of atypical synaptic density in ASD could potentially be a downstream effect of this genetic susceptibility [54, 110, 127]. In mice, behavioural atypicalities have been observed in association with altered mTOR-signalling and deficient autophagy in this pathway [122, 124]. Additionally, altered microglial activity has been associated to long-range connectivity, suggesting another potential cellular underpinning [121, 124].

In effect, these alterations may be associated with local overconnectivity while not ensuring reliable long-range information relay [116, 122]. While speculative, our results potentially suggest a differential impact of pruning between long- and short-range connections, specifically, a higher requirement for longer connections to be retained in autism. Further research contextualizing imaging findings to cellular patterns reflecting on pruning mechanisms is needed to further explore this phenomenon. Histological investigations of cell architecture and microglial activity are necessary to investigate whether findings from animal studies translate to humans, and could thus substantially contribute to a more detailed understanding of differential neurodevelopment with regards to neuronal connection length, and the involvement of atypical pruning in the underlying pathomechanism.

Limitations

The present study investigated connectome contractions in ASD, expanding upon previous findings of atypical connectome hierarchy [25]. We analyzed data from an open-access repository, and selected data from three different acquisition sites according to previously established inclusion criteria [25]. As such, the current dataset was considered adequate to address our research question, and previous analyses have conducted several analyses to explore the effect of image quality and motion on findings. On the other hand, we acknowledge that our results warrant further validation upon availability of independent large-scale datasets. Differences in scanning protocols were addressed through state-of-the-art data harmonization protocols preserving variance in terms of age and diagnosis status. We thus acknowledge the heterogeneity of the original data as a potential limitation to the generalizability of our results. One apparent site-dependent caveat is the notable difference in ADOS scores, suggesting substantial behavioral phenotype differences between cohorts or variations in clinical assessment practices. Consequently, further research is necessary to confirm our results regarding the invariance of CD towards symptom severity scales.

ASD is a complex and heterogeneous condition, with important inter-individual variations across diagnosed individuals. In this study, we have presented results based on group differences obtained from comparing ASD to NT individuals to identify an overarching connectivity pattern shift in ASD. While we assessed associations of these findings against age as well as clinical and cognitive measures, we do recognize that there may be complementary strategies for a more targeted assessment of ASD subtypes [8, 108, 128], which may show diverging imaging and clinical phenotypes, and may be associated to different developmental mechanisms.

Additionally, we investigated several potential confounds to our data. Namely, we could confirm the

robustness of our methodology across signal regression in image processing. Moreover, total intracranial volume as a likely influential factor on geodesic distance measurements did not show significant variation between the groups.

ASD is characterized by heterogeneous symptom phenotypes and prevalent comorbidity with other neurodevelopmental conditions, most notably attention deficit-hyperactivity disorder (ADHD). In the present study, we did not examine comorbidities or other conditions with similar symptom profiles. Further research is needed to confirm this association in larger samples, and to also examine the specificity of these brain-behavior associations for autism *vis-à-vis* other neurodevelopmental indications.

Conclusion

In a multicentric cohort of ASD and NT individuals, we calculated connectivity distance measurements to stratify long- versus short-range functional connections. ASD was associated with lower mean functional connection length, with CD reductions appearing invariant to age or symptom severity. As such, CD possibly constitutes a relatively stable marker of ASD-associated connectome reorganization. On the other hand, CD changes were modulated by intelligence measures, specifically, higher CD was associated with higher IQ scores. Thus, our findings point towards contracted connectome profiles as markers for overall impaired cognitive performance. Conceptually, connectome contractions as imaged by CD implicate decreased communication efficiency [32, 47], offering a potential explanation for their potential contribution to general cognitive function in atypical development.

Abbreviations

ABIDE	Autism Brain Imaging Data Exchange
ADHD	Attention Deficit-Hyperactivity Disorder
ADOS	Autism Diagnostic Observation Schedule
ASD	Autism Spectrum Disorder
CD	Connectivity Distance
DAN	Dorsal Attention Network
DMN	Default Mode Network
FC	Functional Connectivity
FPN	Frontoparietal Network
GSR	Global Signal Regression
HCP	Human Connectome Project
HIPAA	Health Insurance Portability and Accountability Act
IQ	Intelligence Quotient
MRI	Magnetic Resonance Imaging
NT	Neurotypical control participants
NYU	New York University Langone Medical Center
PITT	Pittsburgh School of Medicine
rs-fMRI	Resting state-functional MRI
SMN	Somatomotor network
USM	University of Utah School of Medicine
VAN	Ventral Attention Network

Supplementary Information

The online version contains supplementary material available at https://doi.org/10.1186/s13229-024-00616-2.

Supplementary Material 1

Author contributions

CFW: methodology, data analysis, visualization, writing – original draft, VK: methodology, supervision, writing – review and editing, OB: methodology, supervision, writing – review and editing, HJ: methodology, writing – review and editing, YW: methodology, writing – review and editing, SL methodology, writing – review and editing, AN: methodology, writing – review and editing, XC: writing – review and editing, BYP: methodology, data processing, writing – review and editing, MPM: writing – review and editing, ADM writing – review and editing, SV: methodology, writing – review and editing, SJH: methodology, data curation, writing – review and editing, BCB: conceptualization, methodology, writing – review and editing, supervision.

Funding

Dr. Sofie Valk was funded by the Max Planck Institute. Dr. Boris Bernhardt acknowledges research support from the National Science and Engineering Research Council of Canada (NSERC Discovery-1304413), the Canadian Institutes of Health Research (CIHR FDN-154298, PJT-174995, PJT-191853), SickKids Foundation (NI17-039), Azrieli Center for Autism Research (ACART-ACC), BrainCanada (Azrieli Future-Leaders, McConnell Brain Imaging Centre Platform), and the Tier-2 Canada Research Chairs (CRC) program. Dr. Seok-Jun Hong was funded by Basic Science IBS-R0150D1, National Research Foundation of Korea (NRF) from Korea Government (MIST; NRF-2022R1C1C1007095, R5-2023-00217361, RS-2024-00398768). Dr. Bo-yong Park was funded by the Institute for Information and Communications Technology Planning and Evaluation (IITP) funded by the Korea Government (MSIT) (No. 2022-0-00448, Deep Total Recall: Continual Learning for Human-Like Recall of Artificial Neural Networks; No. RS-2021-II212068, Artificial Intelligence Innovation Hub), and the Institute for Basic Science (IBS-R015-D1).

Data availability

No datasets were generated or analysed during the current study.

Declarations

Ethics approval and consent to participate

Ethics approval was acquired for the original studies in the ABIDE repository.

Competing interests

The authors declare no competing interests.

Author details

[1]Multimodal Imaging and Connectome Analysis Laboratory, McConnell Imaging Center, Montreal Neurological Institute, McGill University, Montreal, QC, Canada
[2]Social Neuroscience Lab, Department of Psychiatry and Psychotherapy, University of Lübeck, Lübeck, Germany
[3]Center of Brain, Behavior and Metabolism (CBBM), University of Lübeck, Lübeck, Germany
[4]Department of Neurology and Neurosurgery, McGill University, Montreal, QC, Canada
[5]Department of Data Science, Inha University, Incheon, South Korea
[6]Center for Neuroscience Imaging Research, Institute for Basic Research, Suwon, South Korea
[7]Center for the Developing Brain, Child Mind Institute, New York, USA
[8]Cognitive Neurogenetics Group, Max Planck Institute for Human Cognitive and Brain Sciences, Leipzig, Germany
[9]Department of Biomedical Engineering, Sungkyunkwan University, Suwon, South Korea
[10]Center for Neuroscience Imaging Research, Institute for Basic Science, Suwon, South Korea

Received: 21 April 2024 / Accepted: 14 August 2024
Published online: 11 September 2024

References

1. Maenner MJ, Shaw KA, Baio J, Washington A, Patrick M, Dirienzo M, et al. Prevalence of Autism Spectrum Disorder among children aged 8 years — Autism and Developmental Disabilities Monitoring Network, 11 sites, United States, 2016. MMWR Surveillance Summaries. 2020;69(4):1–12.
2. American Psychiatric Association. Diagnostic and Statistical Manual of Mental Disorders (DSM-5®). 2013.
3. Levy SE, Mandell DS, Schultz RT, Autism. Lancet. 2009;374(9701):1627–38.
4. Lord C, Risi S, Lambrecht L, Cook EH, Leventhal BL, Dilavore PC, et al. The Autism Diagnostic Observation Schedule-Generic: a standard measure of social and communication deficits associated with the spectrum of autism. Springer; 2000. pp. 205–23.
5. Assaf M, Jagannathan K, Calhoun VD, Miller L, Stevens MC, Sahl R, et al. Abnormal functional connectivity of default mode sub-networks in autism spectrum disorder patients. NeuroImage. 2010;53(1):247–56.
6. Ameis SH, Catani M. Altered white matter connectivity as a neural substrate for social impairment in Autism Spectrum Disorder. Masson SpA; 2015. pp. 158–81.
7. Sato W, Uono S. The atypical social brain network in autism: advances in structural and functional MRI studies. Lippincott Williams and Wilkins; 2019. pp. 617–21.
8. Hong SJ, Vogelstein JT, Gozzi A, Bernhardt BC, Yeo BTT, Milham MP, Di Martino A. Toward Neurosubtypes in Autism. Biol Psychiatry. 2020;88(1):111–28.
9. Delbruck E, Yang M, Yassine A, Grossman ED. Functional connectivity in ASD: atypical pathways in brain networks supporting action observation and joint attention. Brain Res. 2019;1706:157–65.
10. Simms ML, Kemper TL, Timbie CM, Bauman ML, Blatt GJ. The anterior cingulate cortex in autism: heterogeneity of qualitative and quantitative cytoarchitectonic features suggests possible subgroups. Acta Neuropathol. 2009;118(5):673–84.
11. Rane P, Cochran D, Hodge SM, Haselgrove C, Kennedy DN, Frazier JA. Connectivity in Autism: a review of MRI connectivity studies. Taylor and Francis Ltd; 2015. pp. 223–44.
12. Hull JV, Dokovna LB, Jacokes ZJ, Torgerson CM, Irimia A, Van Horn JD. Resting-state functional connectivity in Autism Spectrum disorders: a review. Front Psychiatry. 2016;7:205.
13. Glover GH. Overview of functional magnetic resonance imaging. Neurosurg Clin N Am. 2011;22(2):133-9, vii.
14. Fox MD, Raichle ME. Spontaneous fluctuations in brain activity observed with functional magnetic resonance imaging. Nat Rev Neurosci. 2007;8(9):700–11.
15. Gusnard DA, Raichle ME, Raichle ME. Searching for a baseline: functional imaging and the resting human brain. Nat Rev Neurosci. 2001;2(10):685–94.
16. Greicius MD, Krasnow B, Reiss AL, Menon V. Functional connectivity in the resting brain: a network analysis of the default mode hypothesis. Proc Natl Acad Sci U S A. 2003;100(1):253–8.
17. Fox MD, Snyder AZ, Vincent JL, Corbetta M, Van Essen DC, Raichle ME. The human brain is intrinsically organized into dynamic, anticorrelated functional networks. Proc Natl Acad Sci U S A. 2005;102(27):9673–8.
18. Barch DM, Burgess GC, Harms MP, Petersen SE, Schlaggar BL, Corbetta M, et al. Function in the human connectome: task-fMRI and individual differences in behavior. NeuroImage. 2013;80:169–89.
19. Finn ES, Shen X, Scheinost D, Rosenberg MD, Huang J, Chun MM, et al. Functional connectome fingerprinting: identifying individuals using patterns of brain connectivity. Nat Neurosci. 2015;18(11):1664–71.
20. Damoiseaux JS, Rombouts SA, Barkhof F, Scheltens P, Stam CJ, Smith SM, Beckmann CF. Consistent resting-state networks across healthy subjects. Proc Natl Acad Sci U S A. 2006;103(37):13848–53.
21. Yeo BT, Krienen FM, Sepulcre J, Sabuncu MR, Lashkari D, Hollinshead M, et al. The organization of the human cerebral cortex estimated by intrinsic functional connectivity. J Neurophysiol. 2011;106(3):1125–65.
22. Smith SM, Fox PT, Miller KL, Glahn DC, Fox PM, Mackay CE, et al. Correspondence of the brain's functional architecture during activation and rest. Proc Natl Acad Sci U S A. 2009;106(31):13040–5.
23. Mesulam MM. From sensation to cognition. Brain. 1998;121(Pt 6):1013–52.
24. Margulies DS, Ghosh SS, Goulas A, Falkiewicz M, Huntenburg JM, Langs G, et al. Situating the default-mode network along a principal gradient of macroscale cortical organization. Proc Natl Acad Sci U S A. 2016;113(44):12574–9.
25. Hong S-J, Vos De Wael R, Bethlehem RAI, Lariviere S, Paquola C, Valk SL et al. Atypical functional connectome hierarchy in autism. Nat Commun. 2019;10(1).
26. Funakoshi Y, Harada M, Otsuka H, Mori K, Ito H, Iwanaga T. Default mode network abnormalities in children with autism spectrum disorder detected by resting-state functional magnetic resonance imaging. J Med Invest. 2016;63(3–4):204–8.
27. Sripada C, Kessler D, Fang Y, Welsh RC, Prem Kumar K, Angstadt M. Disrupted network architecture of the resting brain in attention-deficit/hyperactivity disorder. Hum Brain Mapp. 2014;35(9):4693–705.
28. Konrad K, Eickhoff SB. Is the ADHD brain wired differently? A review on structural and functional connectivity in attention deficit hyperactivity disorder. Hum Brain Mapp. 2010;31(6):904–16.
29. Benkarim O, Paquola C, Park BY, Hong SJ, Royer J, de Vos R, et al. Connectivity alterations in autism reflect functional idiosyncrasy. Commun Biol. 2021;4(1):1078.
30. Hong S-J, Vogelstein JT, Gozzi A, Bernhardt BC, Yeo BTT, Milham MP, Di Martino A. Toward Neurosubtypes in Autism. 2020. pp. 111 – 28.
31. Oligschläger S, Huntenburg JM, Golchert J, Lauckner ME, Bonnen T, Margulies DS. Gradients of connectivity distance are anchored in primary cortex. Brain Struct Function. 2017;222(5):2173–82.
32. Oligschläger S, Xu T, Baczkowski BM, Falkiewicz M, Falchier A, Linn G, Margulies DS. Gradients of connectivity distance in the cerebral cortex of the macaque monkey. Brain Struct Function. 2019;224(2):925–35.
33. Somogyi P, Tamas G, Lujan R, Buhl EH. Salient features of synaptic organisation in the cerebral cortex. Brain Res Brain Res Rev. 1998;26(2–3):113–35.
34. Muller RA, Shih P, Keehn B, Deyoe JR, Leyden KM, Shukla DK. Underconnected, but how? A survey of functional connectivity MRI studies in autism spectrum disorders. Cereb Cortex. 2011;21(10):2233–43.
35. Supekar K, Uddin LQ, Khouzam A, Phillips J, Gaillard WD, Kenworthy LE, et al. Brain hyperconnectivity in children with autism and its links to social deficits. Cell Rep. 2013;5(3):738–47.
36. Just MA, Cherkassky VL, Keller TA, Kana RK, Minshew NJ. Functional and anatomical cortical underconnectivity in autism: evidence from an FMRI study of an executive function task and corpus callosum morphometry. Cereb Cortex. 2007;17(4):951–61.
37. Just MA, Keller TA, Malave VL, Kana RK, Varma S. Autism as a neural systems disorder: a theory of frontal-posterior underconnectivity. Neurosci Biobehav Rev. 2012;36(4):1292–313.
38. Long Z, Duan X, Mantini D, Chen H. Alteration of functional connectivity in autism spectrum disorder: effect of age and anatomical distance. Sci Rep. 2016;6(1):26527.
39. von dem Hagen EA, Stoyanova RS, Baron-Cohen S, Calder AJ. Reduced functional connectivity within and between 'social' resting state networks in autism spectrum conditions. Soc Cogn Affect Neurosci. 2013;8(6):694–701.
40. Cerliani L, Mennes M, Thomas RM, Di Martino A, Thioux M, Keysers C. Increased functional connectivity between subcortical and cortical resting-state networks in Autism Spectrum Disorder. JAMA Psychiatry. 2015;72(8):767–77.
41. Buch AM, Vertes PE, Seidlitz J, Kim SH, Grosenick L, Liston C. Molecular and network-level mechanisms explaining individual differences in autism spectrum disorder. Nat Neurosci. 2023;26(4):650–63.
42. Bertelsen N, Landi I, Bethlehem RAI, Seidlitz J, Busuoli EM, Mandelli V, et al. Imbalanced social-communicative and restricted repetitive behavior subtypes of autism spectrum disorder exhibit different neural circuitry. Commun Biol. 2021;4(1):574.
43. Haghighat H, Mirzarezaee M, Araabi BN, Khadem A. Functional networks abnormalities in Autism Spectrum Disorder: Age-Related Hypo and Hyper Connectivity. Brain Topogr. 2021;34(3):306–22.
44. Courchesne E, Pierce K. Why the frontal cortex in autism might be talking only to itself: local over-connectivity but long-distance disconnection. Curr Opin Neurobiol. 2005;15(2):225–30.
45. Kana RK, Libero LE, Moore MS. Disrupted cortical connectivity theory as an explanatory model for autism spectrum disorders. Phys Life Rev. 2011;8(4):410–37.
46. Uddin LQ, Supekar K, Menon V. Reconceptualizing functional brain connectivity in autism from a developmental perspective. Front Hum Neurosci. 2013;7:458.
47. Wang Y, Royer J, Park BY, Vos de Wael R, Lariviere S, Tavakol S et al. Long-range functional connections mirror and link microarchitectural and cognitive hierarchies in the human brain. Cereb Cortex. 2022.
48. Larivière S, Weng Y, Vos De Wael R, Royer J, Frauscher B, Wang Z, et al. Functional connectome contractions in temporal lobe epilepsy: Microstructural underpinnings and predictors of surgical outcome. Epilepsia. 2020;61(6):1221–33.

49. Hong SJ, Vos de Wael R, Bethlehem RAI, Lariviere S, Paquola C, Valk SL, et al. Atypical functional connectome hierarchy in autism. Nat Commun. 2019;10(1):1022.
50. Arion D, Unger T, Lewis DA, Mirnics K. Molecular markers distinguishing supragranular and infragranular layers in the human prefrontal cortex. Eur J Neurosci. 2007;25(6):1843–54.
51. Arion D, Horvath S, Lewis DA, Mirnics K. Infragranular gene expression disturbances in the prefrontal cortex in schizophrenia: signature of altered neural development? Neurobiol Dis. 2010;37(3):738–46.
52. Kang HJ, Kawasawa YI, Cheng F, Zhu Y, Xu X, Li M, et al. Spatio-temporal transcriptome of the human brain. Nature. 2011;478(7370):483–9.
53. Casanova MF, El-Baz A, Vanbogaert E, Narahari P, Switala A. A topographic study of minicolumnar core width by lamina comparison between autistic subjects and controls: possible minicolumnar disruption due to an anatomical element in-common to multiple laminae. Brain Pathol. 2010;20(2):451–8.
54. Hutsler JJ, Casanova MF, Review. Cortical construction in autism spectrum disorder: columns, connectivity and the subplate. Neuropathol Appl Neurobiol. 2016;42(2):115–34.
55. Jacot-Descombes S, Uppal N, Wicinski B, Santos M, Schmeidler J, Giannakopoulos P, et al. Decreased pyramidal neuron size in Brodmann areas 44 and 45 in patients with autism. Acta Neuropathol. 2012;124(1):67–79.
56. Casanova MF, van Kooten IA, Switala AE, van Engeland H, Heinsen H, Steinbusch HW, et al. Minicolumnar abnormalities in autism. Acta Neuropathol. 2006;112(3):287–303.
57. von Economo C, Koskinas GN. Die Cytoarchitektonik Der Hirnrinde Des Erwachsenen Menschen. Vienna and Berlin: Julius Springer; 1925.
58. Triarhou LC. The Economo-Koskinas atlas revisited: cytoarchitectonics and functional context. Stereotact Funct Neurosurg. 2007;85(5):195–203.
59. Amunts K, Lepage C, Borgeat L, Mohlberg H, Dickscheid T, Rousseau ME, et al. BigBrain: an ultrahigh-resolution 3D human brain model. Science. 2013;340(6139):1472–5.
60. Lariviere S, Bayrak S, Vos de Wael R, Benkarim O, Herholz P, Rodriguez-Cruces R, et al. BrainStat: a toolbox for brain-wide statistics and multimodal feature associations. NeuroImage. 2023;266:119807.
61. Lariviere S, Paquola C, Park BY, Royer J, Wang Y, Benkarim O, et al. The ENIGMA Toolbox: multiscale neural contextualization of multisite neuroimaging datasets. Nat Methods. 2021;18(7):698–700.
62. Park BY, Kebets V, Lariviere S, Hettwer MD, Paquola C, van Rooij D, et al. Multiscale neural gradients reflect transdiagnostic effects of major psychiatric conditions on cortical morphology. Commun Biol. 2022;5(1):1024.
63. Paquola C, Royer J, Lewis LB, Lepage C, Glatard T, Wagstyl K et al. The BigBrainWarp toolbox for integration of BigBrain 3D histology with multimodal neuroimaging. Elife. 2021;10.
64. Paquola C, De Vos R, Wagstyl K, Bethlehem RAI, Hong SJ, Seidlitz J, et al. Microstructural and functional gradients are increasingly dissociated in transmodal cortices. PLoS Biol. 2019;17(5):e3000284.
65. Yang Y, Zheng Z, Liu L, Zheng H, Zhen Y, Zheng Y, et al. Enhanced brain structure-function tethering in transmodal cortex revealed by high-frequency eigenmodes. Nat Commun. 2023;14(1):6744.
66. Sydnor VJ, Larsen B, Bassett DS, Alexander-Bloch A, Fair DA, Liston C, et al. Neurodevelopment of the association cortices: patterns, mechanisms, and implications for psychopathology. Neuron. 2021;109(18):2820–46.
67. Katsumi Y, Zhang J, Chen D, Kamona N, Bunce JG, Hutchinson JB, et al. Correspondence of functional connectivity gradients across human isocortex, cerebellum, and hippocampus. Commun Biol. 2023;6(1):401.
68. Di Martino A, Yan CG, Li Q, Denio E, Castellanos FX, Alaerts K, et al. The autism brain imaging data exchange: towards a large-scale evaluation of the intrinsic brain architecture in autism. Mol Psychiatry. 2014;19(6):659–67.
69. Valk SL, Di Martino A, Milham MP, Bernhardt BC. Multicenter mapping of structural network alterations in autism. Hum Brain Mapp. 2015;36(6):2364–73.
70. Benkarim O, Paquola C, Park BY, Kebets V, Hong SJ, Vos de Wael R, et al. Population heterogeneity in clinical cohorts affects the predictive accuracy of brain imaging. PLoS Biol. 2022;20(4):e3001627.
71. Saklofske DH, Schoenberg MR. Wechsler Adult Intelligence Scale (all versions). Springer New York; 2011. pp. 2675–80.
72. Ankenman K, Elgin J, Sullivan K, Vincent L, Bernier R. Nonverbal and verbal cognitive discrepancy profiles in autism spectrum disorders: influence of age and gender. Am J Intellect Dev Disabil. 2014;119(1):84–99.
73. Nader AM, Jelenic P, Soulieres I. Discrepancy between WISC-III and WISC-IV Cognitive Profile in Autism Spectrum: what does it reveal about autistic cognition? PLoS ONE. 2015;10(12):e0144645.
74. Hong SJ, Mottron L, Park BY, Benkarim O, Valk SL, Paquola C et al. A convergent structure-function substrate of cognitive imbalances in autism. Cereb Cortex. 2022.
75. Fischl B, Sereno MI, Dale AM. Cortical surface-based analysis. II: inflation, flattening, and a surface-based coordinate system. NeuroImage. 1999;9(2):195–207.
76. Fischl B, Sereno MI, Tootell RB, Dale AM. High-resolution intersubject averaging and a coordinate system for the cortical surface. Hum Brain Mapp. 1999;8(4):272–84.
77. Dale AM, Fischl B, Sereno MI. Cortical surface-based analysis. I. Segmentation and surface reconstruction. NeuroImage. 1999;9(2):179–94.
78. Marcus DS, Harwell J, Olsen T, Hodge M, Glasser MF, Prior F, et al. Informatics and data mining tools and strategies for the human connectome project. Front Neuroinform. 2011;5:4.
79. Van Essen DC, Glasser MF, Dierker DL, Harwell J, Coalson T. Parcellations and hemispheric asymmetries of human cerebral cortex analyzed on surface-based atlases. Cereb Cortex. 2012;22(10):2241–62.
80. Fischl B, FreeSurfer. NeuroImage. 2012;62(2):774–81.
81. Stein JL, Medland SE, Vasquez AA, Hibar DP, Senstad RE, Winkler AM, et al. Identification of common variants associated with human hippocampal and intracranial volumes. Nat Genet. 2012;44(5):552–61.
82. Sargolzaei S, Sargolzaei A, Cabrerizo M, Chen G, Goryawala M, Noei S, et al. A practical guideline for intracranial volume estimation in patients with Alzheimer's disease. BMC Bioinformatics. 2015;16(Suppl 7):S8.
83. Craddock C, Sikka S, Cheung B, Khanuja R, Ghosh SS, Yan CG et al. Towards Automated Analysis of Connectomes: The Configurable Pipeline for the Analysis of Connectomes (C-PAC). Front Neuroinform Conference Abstract: Neuroinformatics. 2013. 2013.
84. Behzadi Y, Restom K, Liau J, Liu TT. A component based noise correction method (CompCor) for BOLD and perfusion based fMRI. NeuroImage. 2007;37(1):90–101.
85. Murphy K, Fox MD. Towards a consensus regarding global signal regression for resting state functional connectivity MRI. NeuroImage. 2017;154:169–73.
86. Fortin JP, Cullen N, Sheline YI, Taylor WD, Aselcioglu I, Cook PA, et al. Harmonization of cortical thickness measurements across scanners and sites. NeuroImage. 2018;167:104–20.
87. Johnson WE, Li C, Rabinovic A. Adjusting batch effects in microarray expression data using empirical Bayes methods. Biostatistics. 2007;8(1):118–27.
88. Fortin JP, Parker D, Tunç B, Watanabe T, Elliott MA, Ruparel K, et al. Harmonization of multi-site diffusion tensor imaging data. Academic Press Inc.; 2017. pp. 149–70.
89. Worsley KJ, Taylor JE, Tomaiuolo F, Lerch J. Unified univariate and multivariate random field theory. NeuroImage. 2004;23(Suppl 1):S189–95.
90. Hochberg Y, Benjamini Y. More powerful procedures for multiple significance testing. Stat Med. 1990;9(7):811–8.
91. Alexander-Bloch AF, Shou H, Liu S, Satterthwaite TD, Glahn DC, Shinohara RT, et al. On testing for spatial correspondence between maps of human brain structure and function. NeuroImage. 2018;178:540–51.
92. Paquola C, Bennett MR, Lagopoulos J. Structural and functional connectivity underlying Gray Matter Covariance: impact of Developmental Insult. Brain Connect. 2018;8(5):299–310.
93. Di Martino A, Fair DA, Kelly C, Satterthwaite TD, Castellanos FX, Thomason ME, et al. Unraveling the miswired connectome: a developmental perspective. Neuron. 2014;83(6):1335–53.
94. Logothetis NK, Pfeuffer J. On the nature of the BOLD fMRI contrast mechanism. Magn Reson Imaging. 2004;22(10):1517–31.
95. Hong SJ, Valk SL, Di Martino A, Milham MP, Bernhardt BC. Multidimensional Neuroanatomical Subtyping of Autism Spectrum Disorder. Cereb Cortex. 2018;28(10):3578–88.
96. Ecker C, Ronan L, Feng Y, Daly E, Murphy C, Ginestet CE, et al. Intrinsic gray-matter connectivity of the brain in adults with autism spectrum disorder. Proc Natl Acad Sci U S A. 2013;110(32):13222–7.
97. Power JD, Cohen AL, Nelson SM, Wig GS, Barnes KA, Church JA, et al. Functional network organization of the human brain. Neuron. 2011;72(4):665–78.
98. Paquola C, Garber M, Frässle S, Royer J, Tavakol S, Rodriguez-Cruces R et al. The Unique Cytoarchitecture and Wiring of the Human Default Mode Network. biorxiv. 2021.
99. Valk SL, Xu T, Margulies DS, Masouleh SK, Paquola C, Goulas A et al. Shaping brain structure: genetic and phylogenetic axes of macroscale organization of cortical thickness. Sci Adv. 2020;6(39).

100. Valk SL, Xu T, Paquola C, Park BY, Bethlehem RAI, Vos de Wael R, et al. Genetic and phylogenetic uncoupling of structure and function in human transmodal cortex. Nat Commun. 2022;13(1):2341.
101. Garcia-Cabezas MA, Zikopoulos B, Barbas H. The Structural Model: a theory linking connections, plasticity, pathology, development and evolution of the cerebral cortex. Brain Struct Funct. 2019;224(3):985–1008.
102. John YJ, Zikopoulos B, Garcia-Cabezas MA, Barbas H. The cortical spectrum: a robust structural continuum in primate cerebral cortex revealed by histological staining and magnetic resonance imaging. Front Neuroanat. 2022;16:897237.
103. Huntenburg JM, Bazin P-L, Margulies DS. Large-scale gradients in human cortical Organization. Trends Cogn Sci. 2018;22(1):21–31.
104. Sancha-Velasco A, Uceda-Heras A, Garcia-Cabezas MA. Cortical type: a conceptual tool for meaningful biological interpretation of high-throughput gene expression data in the human cerebral cortex. Front Neuroanat. 2023;17:1187280.
105. Bannister AP. Inter- and intra-laminar connections of pyramidal cells in the neocortex. Neurosci Res. 2005;53(2):95–103.
106. Palomero-Gallagher N, Zilles K. Cortical layers: Cyto-, myelo-, receptor- and synaptic architecture in human cortical areas. NeuroImage. 2019;197:716–41.
107. Garcia-Cabezas MA, Barbas H, Zikopoulos B. Parallel Development of Chromatin Patterns, Neuron morphology, and connections: potential for disruption in Autism. Front Neuroanat. 2018;12:70.
108. Grove J, Ripke S, Als TD, Mattheisen M, Walters RK, Won H, et al. Identification of common genetic risk variants for autism spectrum disorder. Nat Genet. 2019;51(3):431–44.
109. Trost B, Thiruvahindrapuram B, Chan AJS, Engchuan W, Higginbotham EJ, Howe JL, et al. Genomic architecture of autism from comprehensive whole-genome sequence annotation. Cell. 2022;185(23):4409–e2718.
110. Hutsler JJ, Zhang H. Increased dendritic spine densities on cortical projection neurons in autism spectrum disorders. Brain Res. 2010;1309:83–94.
111. Fair DA, Dosenbach NU, Church JA, Cohen AL, Brahmbhatt S, Miezin FM, et al. Development of distinct control networks through segregation and integration. Proc Natl Acad Sci U S A. 2007;104(33):13507–12.
112. Fair DA, Cohen AL, Power JD, Dosenbach NU, Church JA, Miezin FM, et al. Functional brain networks develop from a local to distributed organization. PLoS Comput Biol. 2009;5(5):e1000381.
113. Dosenbach NU, Nardos B, Cohen AL, Fair DA, Power JD, Church JA, et al. Prediction of individual brain maturity using fMRI. Science. 2010;329(5997):1358–61.
114. Ernst M, Torrisi S, Balderston N, Grillon C, Hale EA. fMRI functional connectivity applied to adolescent neurodevelopment. Annu Rev Clin Psychol. 2015;11:361–77.
115. Hwang K, Hallquist MN, Luna B. The development of hub architecture in the human functional brain network. Cereb Cortex. 2013;23(10):2380–93.
116. Thomas MS, Davis R, Karmiloff-Smith A, Knowland VC, Charman T. The over-pruning hypothesis of autism. Dev Sci. 2016;19(2):284–305.
117. Petanjek Z, Banovac I, Sedmak D, Hladnik A. Dendritic spines: synaptogenesis and synaptic pruning for the Developmental Organization of Brain circuits. Adv Neurobiol. 2023;34:143–221.
118. Kirkland JM, Edgar EL, Patel I, Kopec AM. Impaired microglia-mediated synaptic pruning in the nucleus accumbens during adolescence results in persistent dysregulation of familiar, but not novel social interactions in sex-specific ways. bioRxiv. 2023.
119. Wang L, Ling H, He H, Hu N, Xiao L, Zhang Y, et al. Dysfunctional synaptic pruning by microglia correlates with cognitive impairment in sleep-deprived mice: involvement of CX3CR1 signaling. Neurobiol Stress. 2023;25:100553.
120. Maliske L, Kanske P. The Social Connectome - moving toward complexity in the study of Brain Networks and their interactions in Social Cognitive and Affective Neuroscience. Front Psychiatry. 2022;13:845492.
121. Paolicelli RC, Bolasco G, Pagani F, Maggi L, Scianni M, Panzanelli P, et al. Synaptic pruning by microglia is necessary for normal brain development. Science. 2011;333(6048):1456–8.
122. Tang G, Gudsnuk K, Kuo SH, Cotrina ML, Rosoklija G, Sosunov A, et al. Loss of mTOR-dependent macroautophagy causes autistic-like synaptic pruning deficits. Neuron. 2014;83(5):1131–43.
123. Ouyang M, Cheng H, Mishra V, Gong G, Mosconi MW, Sweeney J, et al. Atypical age-dependent effects of autism on white matter microstructure in children of 2–7 years. John Wiley and Sons Inc.; 2016. pp. 819–32.
124. Kim HJ, Cho MH, Shim WH, Kim JK, Jeon EY, Kim DH, Yoon SY. Deficient autophagy in microglia impairs synaptic pruning and causes social behavioral defects. Mol Psychiatry. 2017;22(11):1576–84.
125. Peca J, Feng G. Cellular and synaptic network defects in autism. Curr Opin Neurobiol. 2012;22(5):866–72.
126. Filipello F, Morini R, Corradini I, Zerbi V, Canzi A, Michalski B, et al. The Microglial Innate Immune receptor TREM2 is required for synapse elimination and normal brain connectivity. Immunity. 2018;48(5):979–91. e8.
127. Hutsler JJ, Love T, Zhang H. Histological and magnetic resonance imaging assessment of cortical layering and thickness in autism spectrum disorders. Biol Psychiatry. 2007;61(4):449–57.
128. Tang S, Sun N, Floris DL, Zhang X, Di Martino A, Yeo BTT. Reconciling dimensional and categorical models of Autism Heterogeneity: a brain connectomics and behavioral study. Biol Psychiatry. 2020;87(12):1071–82.
129. Vos de Wael R, Benkarim O, Paquola C, Lariviere S, Royer J, Tavakol S, et al. BrainSpace: a toolbox for the analysis of macroscale gradients in neuroimaging and connectomics datasets. Commun Biol. 2020;3(1):103.

Publisher's Note